

# Assessment of ERBE clear scene ID by using the collocated AVHRR data

Toshiro Inoue  
Meteorological Research Institute/JMA

## 1. Introduction

Cloud-radiation interactions have been considered as one of the most critical areas in global climate change research. The effect of clouds on the energy budget of the earth is in the way of cooling effect by reflecting solar radiation and warming effect by preventing the earth-emitted long-wave radiation. To study cloud effects on climate, we often use the term of cloud radiative forcing which is defined as the flux difference between cloudy condition and clear condition. We understand that the reliability of cloud radiative forcing is depending on how accurately we can estimate the clear radiance.

In this study, collocated ERBE and AVHRR data are used to compare ERBE short-wave and long-wave fluxes at the top of the atmosphere, and cloud/cloud-free information by AVHRR data within the footprint of the ERBE. The ERBE S-8 data include scene ID which indicates clear, partly cloudy and overcast within a footprint. We used this scene ID for selecting cloud free data for the ERBE data. On the other hand, the spatial uniformity and mean brightness temperature of  $11\ \mu\text{m}$  of AVHRR within the ERBE footprint are used to identify ERBE cloud free scene. To assess these clear scene ID and clear scene determined from AVHRR we compared with visible reflectivity and short-wave fluxes .

## 2. Data

This study makes use of collocated AVHRR and ERBE observations made from the NOAA-9 polar orbiting satellite, over the eastern Pacific (15S-35S, 75W-100W) for the years 1985 and 1986. The NOAA-9 nominal equator crossing times are 0900 UTC and 2100 UTC.

The AVHRR data used in this study is the Global Area Coverage (GAC) data which has a nominal resolution at nadir of 4 km. The AVHRR has five spectral bandpasses: Channel 1 (0.56-0.68  $\mu\text{m}$ ); Channel 2 (.725-1.1  $\mu\text{m}$ ); Channel 3 (3.55-3.93  $\mu\text{m}$ ); Channel 4 (10.3-11.3  $\mu\text{m}$ ); and Channel 5 (11.5-12.5  $\mu\text{m}$ ). These five channels are located in spectral regions where atmospheric gases are characterized by weak absorption. The AVHRR data are therefore good for studying surface properties, such as sea surface temperature and vegetation properties, and cloud top properties. Inoue (1987) developed a cloud type classification, referred to as the split window technique, based on the equivalent brightness temperature in Channel 4 (BT11) and the temperature difference between Channel 4 and 5 (BTD). The BTD is essential to classify cloud free, optically thin cirrus and optically thick clouds.

ERBE observations are used to specify the broadband energy budget at the top of the atmosphere. At nadir the ERBE footprint is approximate 35 km. The ERBE scanning instrument has been discussed by Kopia (1986). The method of inverting the instantaneous scanner observations to the top of the atmosphere fluxes is discussed in Barkstrom et al (1989), and Smith et al (1986).

Collocation of the AVHRR pixels with the ERBE footprint is accomplished based on the method developed by Ackerman et al. (1992), Ackerman and Inoue (1994). The method is based on the scanning geometry of both instruments.

## 3. Clear Data Analysis

The first step is to determine the clear-sky thresholds of brightness temperature for  $11\ \mu\text{m}$ (BT11) and brightness temperature difference between the  $11\ \mu\text{m}$  and  $12\ \mu\text{m}$ (BTD) for each  $2.5\times 2.5$  latitude/longitude region within the area of study. This is accomplished through analyze of  $3\times 3$  groups of AVHRR pixels. In step 1, a first guess threshold of BT11 is determined using the spatial coherence approach of Coakley and Bretherton (1982). The spatial coherence method is used to estimate the clear-sky thresholds for BT11, specified as the foot of the 'foot' of the clear-sky arch.

In the second pass through the data, only those  $3\times 3$  groups of pixels that have a standard deviation less than  $0.4\text{C}$  and a mean BT11 that is greater than the initial threshold selected by

the spatial coherence analysis are considered. Each group of AVHRR pixels is assigned an appropriate 2.5 by 2.5 degree grid box. The mean BT11 and mean BTD for each grid box are then computed and assigned the clear-sky thresholds values.

Having selected a clear-sky threshold that is a function of month and geographic region, a third pass through the data is made. In this final pass, each individual AVHRR pixel that lies within and ERBE footprint is classified using the predetermined clear BT11 and BTD according to the split window technique.

#### 4. Results

The clear scene ID is compared with the average visible reflectivity computed from collocated AVHRR pixels. The clear scene determined from the collocated AVHRR is also compared with the visible reflectivity. In determination of cloud free footprint, only infrared data is used as was stated before. Figure 1-a shows the bivariate histogram for scene ID and visible reflectivity. The scene ID of 10 indicates cloud free, and 60 indicates partly cloudy. We can see most of the clear scene ID indicates the visible reflectivity is less than 5%. Same features are seen in Figure 1-b for the data which cloud cover within the footprint is less than 5%. However, there are some data for the higher visible reflectivity even for the clear scene ID and the cloud cover less than 5%, although cloud cover less than 5% shows smaller number of data than that of clear scene ID.

Figure 2 shows scatter plots of visible reflectivity and scene ID for the data of January in 1986 (b) and other date(a). Figure 3 shows scatter plots of visible reflectivity and cloudiness(%). We can see relatively higher visible reflectivity for both clear scene ID and cloud cover less than 5% for the case of January in 1986. Other data show much lower visible reflectivity than this. We simply consider that some bad data are included for the data in January. Further study is required to study this reason. Generally speaking, both scene ID and cloud cover less than 5% show reasonable agreement with visible reflectance.

Figure 4 shows the short-wave flux ( $W/m^2$ ) and long-wave flux ( $W/m^2$ ) at the top of the atmosphere retrieved from ERBE observations for the clear scene ID (a) and clear scene by AVHRR (b). This indicates smaller SW for the cloud cover less than 5% than clear scene ID. This suggest the use of AVHRR shows less contaminated with clouds.

Figure 5-a represents the histogram of cloud cover determined from the collocated AVHRR for the clear scene ID footprint. This means most of clear scene ID corresponds to cloud cover is less than 10% but some are contaminated by cloud up to 100% by the cloud cover estimate from collocated AVHRR. The higher cloud cover might be caused by optically thin cirrus clouds. Figure 5-b shows the histogram of scene ID (10 is clear and 60 is partially cloudy) for the ERBE footprint which is covered by cloud less than 5% determined from collocated AVHRR data. The 90% of the clear scene determined by AVHRR agree with clear scene ID of 10.

#### 5. Summary

The reliability of cloud radiative forcing is depending how clear data is accurate, since the cloud radiative forcing is defined as the flux difference between cloudy conditions and clear conditions. The clear scene of ERBE footprint is determined from collocated AVHRR infrared data. This clear ERBE footprint is compared with clear scene ID assigned by ERBE. The clear scene ID and clear scene which is determined by AVHRR show reasonable agreement in terms of both smaller visible reflectivity and smaller shortwave flux generally. However, the use of collocated AVHRR indicates better results, since it indicates which shows smaller short-wave fluxes (less contaminated with cloud).

#### References

- Ackerman, R., A. Frey, and W. L. Smith, 1992: Radiation budget studies using collocated observations from AVHRR, HIRS/2 and ERBE instruments. *J. Geophys. Res.* 97, 11 513-11 525.
- Ackerman, S. A. and T. Inoue, 1994: Radiation energy budget studies using collocated AVHRR and ERBE observations. *J. Appl. Meteor.*, 33, 370-378
- Barkstrom, B. R., E. F., Harrison, G. Smith, R. Green, J. Kebler, R. Cess, and the ERBE Science Team, 1989: Earth Radiation Budget Experiment (ERBE) archival and April 1985 results. *Bull. Amer. Meteor. Soc.*, 70, 1254-1262.
- Inoue, T., 1987: A cloud type classification with NOAA-7 split window measurements. *J. Geophys. Res.*, 92, 3991-4000
- Kopia, L. P., 1986: Earth radiation budget experiment scanner instruments. *J. Geophys. Res.*, 24, 400-406.
- Smith, G. L., R. N. Green, E. Raschke, L. B. Avis, J. T. Suttles, B. A. Wielicki, and R. Davies, 1986: Inversion methods for satellite studies of the earth's radiation budget: Development of algorithms for the ERBE mission. *Rev. Geophys.*, 24, 407-421.

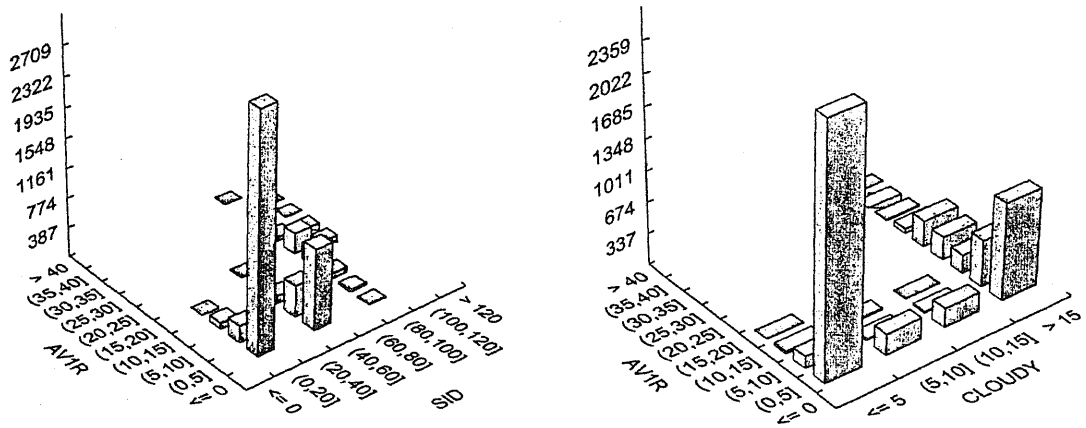


Figure 1-a(left), -b(right). The bivariate histogram for scene ID and visible reflectivity (left) and cloudiness(%) by collocated AVHRR (right).

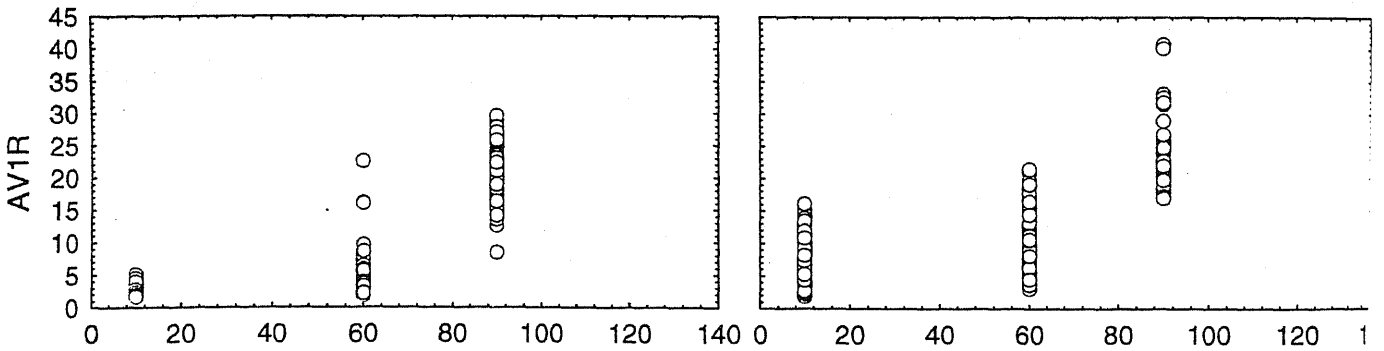


Figure 2 The scatter plots of visible reflectivity and scene ID for the data of January in 1986 (b) and other date(a).

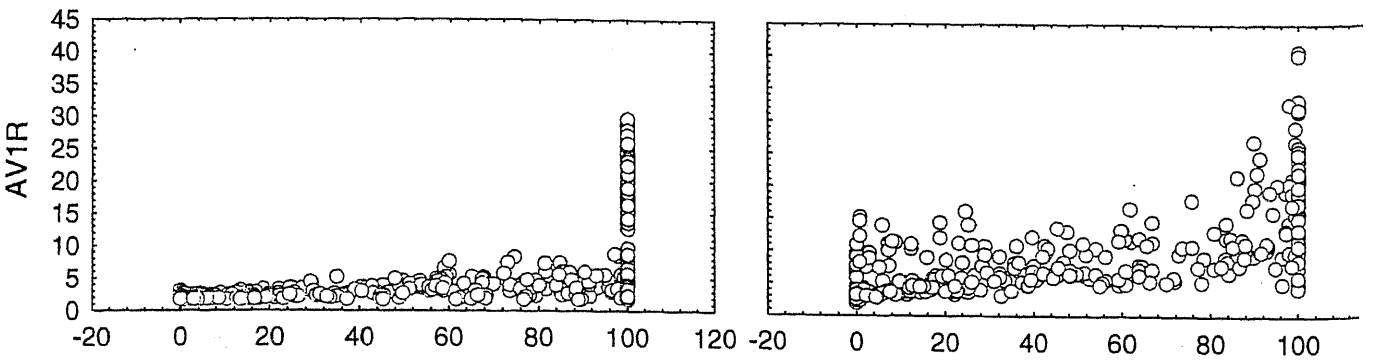


Figure 3 The scatter plots of visible reflectivity and cloudiness(%) for the data of January in 1986 (b) and other date(a).

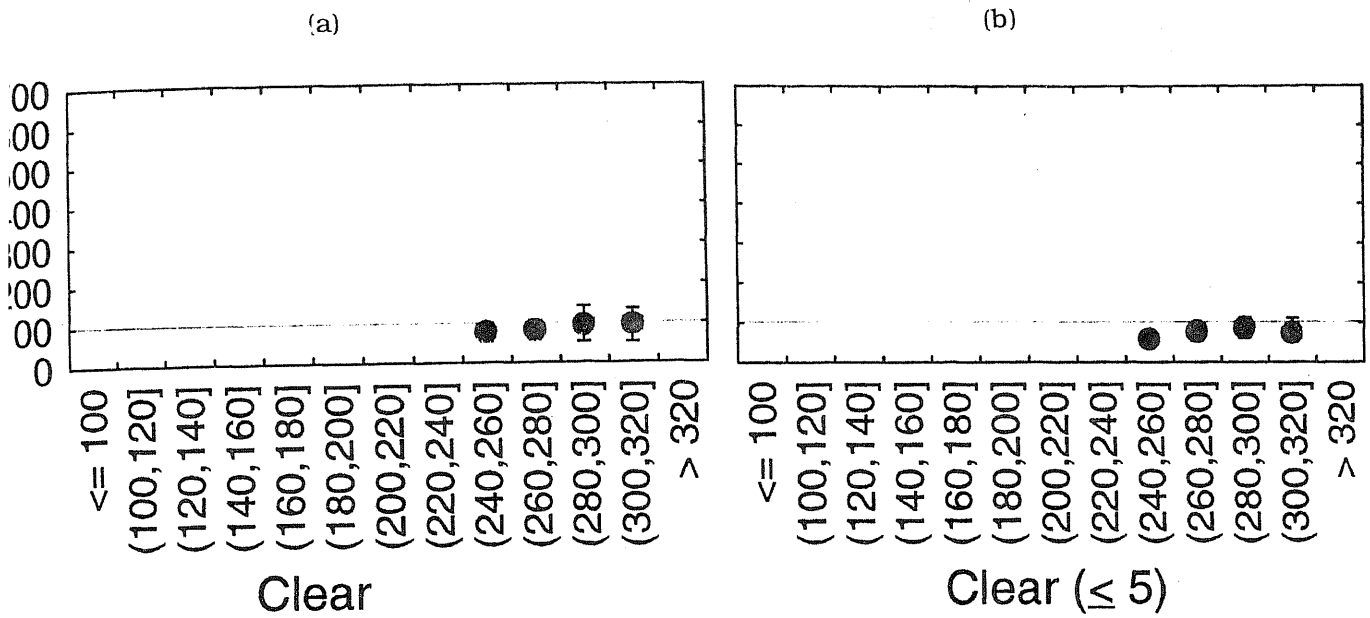


Figure 4 The short-wave flux ( $W/m^2$ ) and long-wave flux ( $W/m^2$ ) at the top of the atmosphere retrieved from ERBE observations for the clear scene ID (a) and clear scene by AVHRR (b).

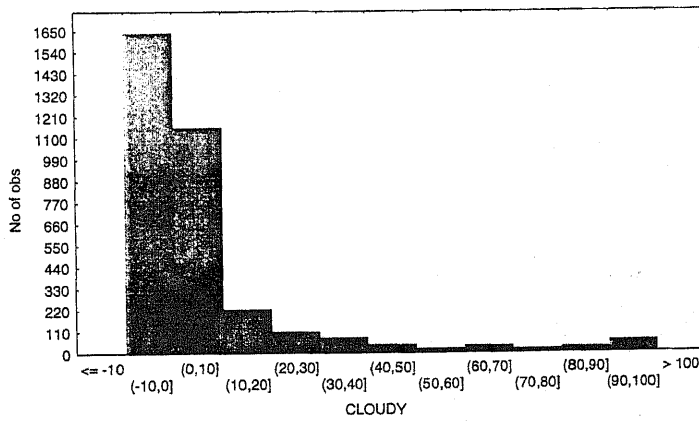


Figure 5-a The histogram of cloud cover determined from the collocated AVHRR for the clear scene ID footprint.

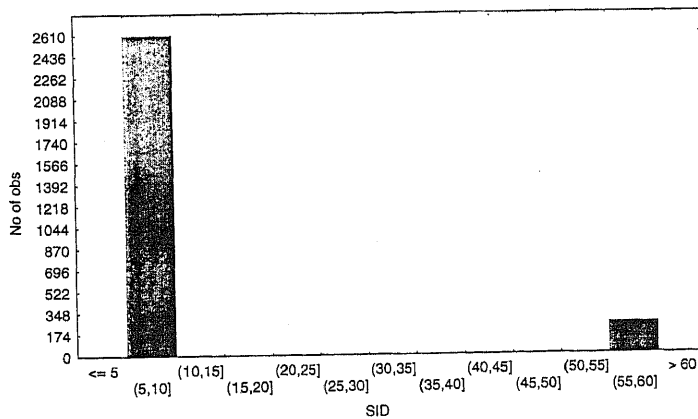


Figure 5-b The histogram of scene ID (10 is clear and 60 is partially cloudy) for the clear ERBE footprint which is covered by cloud less than 5% determined from collocated AVHRR data.